

# **Optimization of Ash and Energy Yields from the Combustion of Flamboyant Pod, Groundnut Shell and Additive (Kaolin) Composite**

## **ABSTRACT**

**Aim:** I-optimal design via the Combined Methodology of the design expert software was used to optimize the ash yield from the combustion of a biocomposite mixture of Flamboyant Pod and Groundnut Shell with additive (Kaolin) in a grate furnace.

**Study Design:** Analysis of Variance, and Artificial Neural Network were used to predict the ash yield from the data generated from the design process, while the coefficient of determination between variables was determined using the Principal Coefficient Analysis. The resulting ash yield was characterized for ash composition using a Scanning Electron microscope.

**Place and Duration of Study:** Biochemical Engineering Laboratory, Department of Chemical Engineering, Ladoke Akintola University of Technology, Ogbomoso. September-December 2020.

**Methodology:** Proximate analysis was used to determine Moisture Content, Fixed Carbon Content, and Volatile Matter values used to determine the Higher Heating Value of the composite.

**Results:** The sample with 53% Flamboyant Pod, 37% Groundnut Shell, and 10% kaolin mixture at 825 °C gave the lowest ash yield of 5%. The correlation coefficient ( $R^2$ ) of the model equation developed for ash yield (0.9992) validated the model due to its closeness to 1. The deviation between the experiment and prediction for ash yield indicated 3%. The Higher Heating Value calculated shows that the lowest ash yield composition has a higher heating value of 15.14 and the highest yield mixture has a lower Higher Heating Value of 12.26.

**Conclusion:** The reduction of ash yield from 56% to 5% (as observed in previous studies shows a greater improvement in ash reduction during the combustion process.

**Keywords:** Ash, Biomass, Solid Fuel, Renewable energy

## ABBREVIATIONS

ANN	Artificial Neural Network
ANOVA	Analysis of Variance
CM	Combined Methodology
DOD	D-optimal Design
DOE	Design of Experiment
FBM	Feed Biomass Mixture
FCC	Fixed Carbon Content
FP	Flamboyant Pod
GNS	Groundnut shell
HHV	Higher Heating Value
MC	Moisture Content
MSE	Mean Square Error
PCA	Principal Component Analysis
RMSE	Root Mean Square Error
SEM	Scanning Electron microscope
VM	Volatile Matter

## 1. INTRODUCTION

Energy scarcity and environmental pollution are major global issues. The present uncertainty in the world for fuel supply and projected increase in demand brings about the search for alternative sources of fuel which will be cleaner, cheaper and readily accessible. Biomass is a carbon-neutral energy source (substance) of plant and animal origin as well as any type of biological waste from agricultural, industrial, and municipal activities [1]. Biomass is one of the earliest sources of energy, especially in rural areas where it is often the only accessible and affordable source of energy[2]. It can be obtained from conventional crops, agricultural residue, or domestic or industrial waste. Biomass can be converted into liquid, solid and gaseous fuels with the help of some physical, chemical, and biological conversion processes [3].

Ash deposition, poor ignition and combustion temperature reduction have been identified as some of the challenges faced during biomass combustion in large-scale utilization of biomass for power/heat generation, thus the reduction of ash formation and aggregation during biomass combustion among others has become a point of interest in the biomass-based renewable energy industry [4] as this will ensure efficient and clean combustion of biomass. The use of additives such as kaolin during the combustion process is one of the means of solving some of these challenges [5]. High moisture content can lead to poor ignition and reduction of combustion temperature, which in turn hinders the combustion of the reaction products and consequently affects the quality of combustion. In addition, the presence of alkaline metals in solid biofuel causes the formation of complex eutectic salts and consequently lowers the melting temperature of the ashes during combustion [6]. The ash content in biomass is commonly measured gravimetrically by burning samples in a muffle furnace at a high temperature for a specified duration [7].

Combustion additives have been used before in boilers to enhance combustion efficiencies and reduce emissions of Carbon Monoxide, hydrocarbons, particulates, NO<sub>x</sub>, and SO<sub>2</sub>, as well as control agglomeration, fouling, slagging, and corrosion [8]. Combustion additives are solid, liquid, or gaseous substances, that can change the physical and/or chemical characteristics of fuel to achieve some of the above-mentioned results [9].

Biomass has been utilized, largely, as a precursor in many manufacturing processes. In a study on the evaluation of binders in the production of briquettes, empty fruit bunches of *Elais Guinensis* were used as a binder in briquette production [10]. Chin and Paridah (2015) investigated the reduction of ash-related operation problems of fast-growing timber species and oil palm biomass for combustion application[4]. Some ash-related operation problems were identified in the study. The optimization of the oil extraction process from coconut using response surface methodology has been investigated and the ash yield from the combustion of the biomass used was determined[11], while Kareem *et al.* (2018) investigated the optimization of ash yield during the combustion of palm kernel-based biofuel[12].

Flamboyant tree plantation is cultivated worldwide for its ornamental reasons and preservation of soil. It grows freely and vastly in major parts, especially the Rain Forest and Savannah Regions. They produce hardy pods which are mostly left to litter and rot in the vicinity of the parent tree and as such may be a very interesting precursor for the production of energy due to their abundance [13]. Groundnut is a nutritious leguminous crop, grown mainly for seed and oil worldwide. GNS is the leftover obtained after the removal of groundnut seed from its pod. GNS is considered agro-industrial residue and every year

millions of tons of its quantity are left in the environment. These shells undergo slow degradation in a natural environment due to their rich lignin [14]. This study was aimed at evaluating the ash yield during the combustion of the mixture of FP, GNS and Kaolin (as additive), while the data obtained were modeled via Artificial Neural Network and Principal Component Analysis.

## 2. METHODOLOGY

### 2.1 Materials Processing

The GNS was obtained from local markets in Ogbomoso, Nigeria, while the FP was obtained from the LAUTECH Teaching and Research Farm, LAUTECH, Ogbomoso, Nigeria, the two materials were washed severally with water and thoroughly rinsed with distilled water to remove any soluble materials attached, then sun-dried. They were crushed and milled to grain sizes and finally sieved to a uniform size (1 mm). The additive used was Kaolin, which is of analytical grade and was obtained from a reliable supplier to the manufacturer. All the equipment used was well-calibrated before use.

### 2.2 Experimental Design

D-optimal Design (DOD) under Combined Methodology (CM) of the Design-Expert Software (12.0.1.0) was used to optimize the mixture of the component and process factors. The minimum and maximum levels of the components (FB, GNS, and Kaolin) are in the range of 50-60, 35-40 and 5-10%, respectively, while the factor level is in the range of 600-900°C (Table 1). The software gave twenty Experimental Runs which is a mix of the additive and components in various percentages but all aggregated to 100% at each experimental run for the various temperatures suggested [12].

**Table 1. Selected factors and their levels for the design**

Input Variables	Details			Levels	
	Code	Name	Units	Low	High
Components	A	Flamboyant Pod	%	50	60
	B	GNS	%	35	40
	C	Kaolin	%	5	10
Factors	D	Temperature	°C	600	900

### 2.3 Determination of ash yield in the mixture of FB, GNS, and additive

The FB, GNS, and kaolin were ashed according to the ASTM E1755-01 [15]. The oven-dry weight (ODW) and the percentage ash content were determined according to Eqns. 1 and 2, respectively [5].

$$ODW = \frac{Weight_{air-dried\ sample} \times Total\ Sample}{100} \quad (1)$$

$$\%Ash = \frac{Weight_{crucible} + ash - Weight_{crucible}}{ODW} \quad (2)$$

## 2.4 Data Analysis

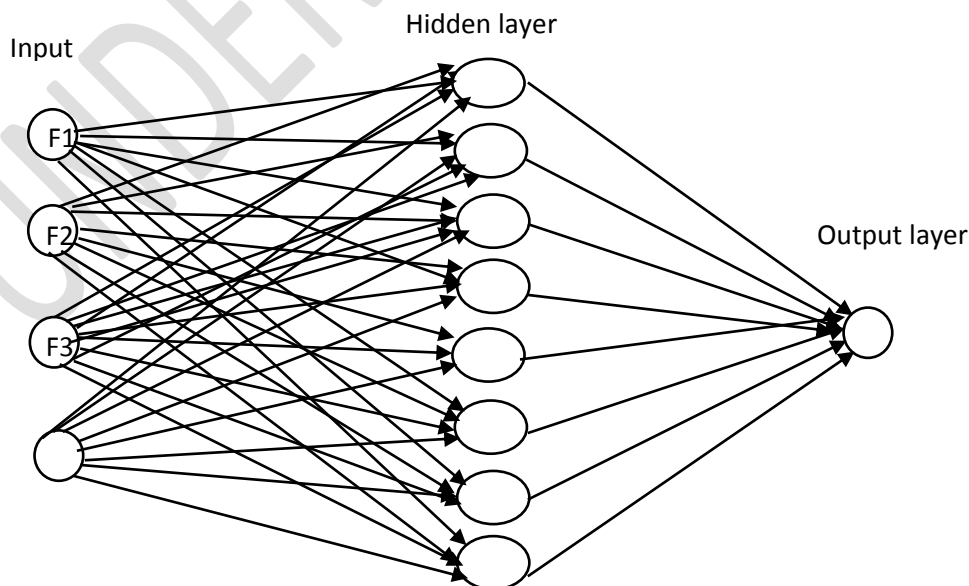
Design Expert analytical tool was used for Analysis of Variance (ANOVA) and validation of the quality of fit of the models generated. The design ratios given by DOE were inserted into the Artificial Neural Network (ANN) for the prediction of ash yield. Principal Component Analysis (PCA) was used to determine the correlation coefficients between variables.

### 2.4.1 Optimizations

The stated analyses were carried out to determine the quality of fit of the models generated using multiple coefficients of determination  $R^2$ , residual sum of square errors for optimal parameters' coefficient fitness based on a linear mixture of the parameters with higher  $R^2$ . In addition, significance difference tests at a level of 10% ( $p < 0.1$ ) and F value were also carried out using the analysis of variance (ANOVA) tool in the Design-Expert Software environment.

### 2.4.2 Neural network modeling (ANN)

Neural Network Toolbox V15.0 of MATLAB mathematical software was used to predict the ash yield of biomass mixture during the combustion process. Multiple Layer Perception (MLP) based on feed-forward ANN was applied to build the predictive model for the pilot plant. The network consists of four (4) input layers, six hidden layers, and one output layer (Figure 1). The inputs for the network are flamboyant pod, groundnut shell, kaolin, and temperature. Output is the percentage ash yield. The performance of the network was measured using the coefficient of correlation (R), the MSE, the Coefficient of Determination ( $R^2$ ), and the RMSE. The network was trained using the Levenberg-Marquardt backpropagation algorithm while the transfer function used was sigmoid Symmetric (tansig) for the hidden layer and purelin for the output layer. The experimental data employed in the ANN Design is shown in Table 2.



F1= Flamboyant, F2 = GNS, F3=Kaolin F4= Ash yield

Fig.1.Scheme of the Artificial Neural Network used as the Numerical Model

Table 2: Experimental Data Employed in ANN Design

Input 1 (%)	Input 2 (%)	Input 3 (%)	Input 4 (%)	Target (%)
58	35	7	818	24
51	40	9	600	66
54	38	8	900	20
59	36	5	600	60
54	40	6	821	15
54	40	6	900	35
50	40	10	888	33
55	40	5	606	55
53	37	10	825	5
60	35	5	752	56
55	35	10	671	37
56	39	5	675	70
54	38	8	750	9
56	35	9	675	15
51	39	10	900	18
58	35	7	749	57
54	38	8	600	80
56	39	5	900	20
56	37	7	900	63
58	37	5	747	55

### **2.4.3 Principal component analysis**

Data were entered into MATLAB (version 15) and a PCA was conducted on the 20 runs, using a direct (oblique) rotation to obtain a parsimonious solution by explaining the variation in the original data set using a few underlying components [16]. Item-to-subject ratios met the recommendations for sample size with the use of pairwise deletion for missing data. Reliability tests of Kaiser–Meyer–Olkin (KMO) measure sampling adequacy and communality values justified the use of the PCA.

## **2.5 Proximate and Energy Content Analysis**

Proximate analyses were carried out according to the ASTM E870-82 standard test methods [17]. The mixture of FB, GNS and kaolin additive was considered a suitable mix for the furnace and thus characterized as the FBM. The mixture of FB, GNS, and kaolin that gives the lowest and highest ash yield was further analysed for proximate analysis, where the MC, FCC, and VC were determined as well as its heating value.

### **2.5.1 Moisture content**

The FBM (10 g) was weighed into a previously dried (105 °C) and weighed crucible. The mixture was then oven-dried at 80 °C overnight, after which it was cooled in a desiccator to room temperature and then re-weighed. The percentage moisture content was determined according to Eqn 3.

$$\% \text{ Moisture Content} = \frac{\text{Wet Sample} - \text{Dry Sample}}{\text{Dry Sample}} \times 100 \quad (3)$$

### **2.5.2 Volatile content**

The FBM sample was placed in a crucible and placed in a muffle furnace at 550 °C for 30 mins. The dish and sample were cooled in a desiccator and weighed. The total volatile contents concentration was calculated using the expression in Eqn 4.

$$\text{volatile contents} = (R - A) \times \frac{100}{\text{sample weight}} \quad (4)$$

Where, R = the weight of the crucible and sample before ignition and A = the weight of the crucible and sample after ignition.

### **2.5.3 Fixed carbon content**

The carbon content of the FBM was determined by heating this blend in a standard crucible with a burner, in such a way that the vapour produced was burned up within 30 mins.

### **2.5.4 Higher heating value estimation**

The higher heating values (HHV) were calculated for the FBM using the standard method. The HHV for the samples was predicted using the correlation in Eqn 5 [18].

$$HHV = 0.1905V + 0.2521FC \quad (5)$$

## 2.6 Determination of FBM Morphology

Scanning Electron Microscopy (SEM) was used in the study to visualise the morphology of the FBM sample [19]. The FBM sample was mixed with Potassium Bromide and placed in the SEM machine at an accelerating voltage of 10KV and 20 kV while the magnification used was between 100 X (500  $\mu\text{m}$ ) – 10000 X (5  $\mu\text{m}$ ) [20].

## 3. RESULTS AND DISCUSSIONS

### 3.1 Optimization of Ash Yield

D-Optimal Design (DOD) under the Combined Methodology under the Design Expert software (12.0.1.0) was employed to optimize the percentage composition of the mixture and process factor (temperature). The maximum ash yield of 81% was obtained from experimental Run 20 (58% FB, 37% GNS, and 5% kaolin at 600 °C) while Run 9 (53% FB, 37% GNS, and 10% kaolin at 825 °C) gave the lowest ash yield (Table 2). The percentage composition of the two Experimental Runs (Run 2 and Run 9) are almost similar. The disparity, though increased for Run 9, indicated that an increase in the addition of the kaolin led to a reduction in the ash yield and this is the primary justification of this study. Thus Run 9 has the lowest ash yield, therefore it was considered the optimum FB, GNS-additive mixture. Run 20 gave the highest yield (81%) of ash, and this is not desirable because the combination will decrease the combustor utilization efficiency and increase the corrosion potential of the reactor [21]. Table 3 shows the Experimental Design Matrix for D-Optimal Design (DOD) with the respective number of runs.

**Table 3: Experimental design matrix for D-Optimal design (DOD)**

Run	Component Mixture (%)			Factor	Response
	Flamboyant Pod	Groundnut Shell	Kaolin	Temperature (°C)	Ash Yield (%)
1	58	35	7	818	24
2	51	40	9	600	66
3	54	38	8	900	20
4	59	36	5	600	60
5	54	40	6	821	15
6	54	40	6	900	35
7	50	40	10	888	33
8	55	40	5	606	35

9	53	37	10	825	5
10	60	35	5	752	56
11	55	35	10	671	37
12	56	39	5	675	70
13	54	38	8	750	9
14	56	35	9	675	15
15	51	39	10	900	18
16	58	35	7	749	57
17	54	38	8	600	80
18	56	39	5	900	20
19	56	37	7	900	63

### 3.2 Model Summary Statistics for the Response

Correlation and multiple regression analyses were conducted to examine the relationship between biomass mixture and ash yield. Table 4 shows the combined model statistics summary. The quadratic-quadratic model was suggested for the mixture-factor relationship on the response (ash yield), because of the highest  $R^2$  values of 1.000 and since other models were aliased, they are unfit for selection and thus they were rejected[22].

**Table 4: Combined model fit summary**

Mixture Order	Process Order	Mixture p-value	Process p-value	Adjusted $R^2$	Predicted $R^2$
M	L	NC	0.0314	0.2001	0.0858
M	Q	NC	0.1673	0.2484	0.1010
M	C	NC	0.4898	0.2242	-0.0109
L	M	0.1110	NC	0.1453	-0.0201

L	L	0.5007	0.3456	0.1775	-0.1514
L	Q	0.1053	0.0438	0.5080	0.0652
L	C	0.2610	0.6843	0.4245	-1.3510
Q	M	0.8209	NC	0.0174	-0.5424
Q	L	0.8043	0.5982	-0.0816	-1.5119
<b>Q</b>	<b>Q</b>	<b>0.0021</b>	<b>0.0014</b>	<b>1.0000</b>	<b>0.9992*</b>
SC	M	0.2406	NC	0.0555	-0.5844^
SC	L	0.7811	0.8261	-0.3717	-6.1057^
C	M	0.6986	NC	-0.0830	-1.6095^

M is Means, L is Linear, Q is Quadratic, SC IS Special Cubic and C is Cubic, NC – NotCalculated, \* Suggested and ^ Aliased

### 3.3 Development of the Regression Model Equation for the Responses

The model equation that was used for identifying the interaction of the factor is expressed in Eqn 6. Ash yield is an objective function and the negative value signifies the parameter that cannot be raised, while the positive sign indicates the parameter that can be increased to achieve the desired objective function. The final model equation was developed in terms of coded factors for ash yield quadratic models obtained for accurate prediction of ash produced (yield) from the mixture of FB, GNS, and selected additive in terms of coded factors generated under Design Expert Software is expressed below. The equation also indicates the presence of linear, square, and crossed terms for the variable investigated.

$$\begin{aligned} \text{Ash yield} = & 7.27A + 6.98B + 56.97C + 3.34AB - 60.44AC + 16.20AD - 139.11BC - 20.84BD - \\ & 24.37CD + 14.83ABD - 26.23ACD + 86.68BCD + 5.32AB^2 - 123.84BD^2 - 117.77CD^2 + \\ & 240.41ABD^2 - 13.25ACD^2 + 533.51BCD^2 \end{aligned} \quad (6)$$

Where A= Flamboyant Pod, B= Groundnut Shell, C = kaolin and D = temperature.

The equation has positive coefficients of +7.27, +6.98, + 56.97, +3.34, +14.83, +86.68, +5.32, and +533.51 obtained for A, B, C, AB, AD, ABD, BCD, AB<sup>2</sup>, ABD<sup>2</sup> and BCD<sup>2</sup> as well as negative coefficients - 60.44, -139.11, -20.84, -24.37, -26.23, -123.84, -117.77, and -13.25 obtained for AC, BD, CD, ACD, BD<sup>2</sup>, CD<sup>2</sup>, and ACD<sup>2</sup> indicate the positive and negative influences of the variable(%Flamboyant Pod, %Groundnut Shell, % kaolin and temperature) on the ash yield [23].

### 3.4 Analysis of Variance (ANOVA) for Ash Yield

The significance of any process parameter can be stated by the corresponding Fisher statistical test(F-test) value of the AVOVA study. For a parameter to be significant, the F-value should be higher and the P-value (probability value) should be less than 0.05 at a 95% confidence interval [24]. The Analysis of

Variance (ANOVA) of the data obtained for percentage ash yield was presented in Table 5. The high model F-value of 268199.28 obtained for ash yield implies that the model is significant and there was only a 0.15% chance that a “Model F-value” of this magnitude has occurred due to noise. Similarly, Model terms AB, AC, AD, BC, BD, and CD, were also significant (Table 5). [23].

The outcomes indicated that the generated linear mixture models' coefficients were highly adequate in close-fitting the experimental results at 0.0005 for ash yield (Table 5). Generally, values of “prob >F” less than 0.05 indicated that the model term was significant while values greater than 0.5 indicated that the model terms were not significant. In this case, A, B, C, and AB, etc. are significant model terms.

**Table 5. Analysis of variance (ANOVA) and regression statistical parameters for ash yield**

Source	Sum of Squares	Df	Mean Square	F-value	p-value Prob>F
<b>Model</b>	72.13	17	4.24	2.682E+05	0.0015*
<sup>(1)</sup> Linear Mixture	17.33	2	8.67	5.477E+05	0.0010*
AB	0.0309	1	0.0309	1952.84	0.0144*
AC	9.32	1	9.32	5.892E+05	0.0008*
AD	8.75	1	8.75	5.531E+05	0.0009*
BC	8.35	1	8.35	5.281E+05	0.0009*
BD	1.87	1	1.87	1.184E+05	0.0018
CD	1.61	1	1.61	1.015E+05	0.0020
ABD	0.2874	1	0.2874	18166.88	0.0047
ACD	0.4326	1	0.4326	27341.88	0.0038
BCD	6.35	1	6.35	4.013E+05	0.0010
AD <sup>2</sup>	1.21	1	1.21	76299.12	0.0023
BD <sup>2</sup>	10.73	1	10.73	6.781E+05	0.0008
CD <sup>2</sup>	8.30	1	8.30	5.244E+05	0.0009
ABD <sup>2</sup>	10.23	1	10.23	6.464E+05	0.0008
ACD <sup>2</sup>	0.0937	1	0.0937	5921.85	0.0083

BCD <sup>2</sup>	13.65	1	13.65	8.626E+05	0.0007
<b>Residual</b>	0.0000	1	0.0000		
<b>Cor Total</b>	72.13	18			
Standard Deviation	0.40		R <sup>2</sup>	1.0000	
Mean	6.08		Adjusted R <sup>2</sup>	1.0000	
C.V	6.55		Predicted R <sup>2</sup>	0.9992	
PRESS	5.71		Adequate Precision	1718.3635	

A=Flamboyant pod, B=GNS, C=Kaolin=Temperature \*Significant @ p<0.05

### **3.4.1 Experimental response to the regression statistics**

From the statistical parameters for the outputs recorded in Table 5, the estimated correlation coefficient (R<sup>2</sup>) of the model equation developed for ash yield is 1.0000, this value is in reasonable agreement with the predicted R<sup>2</sup> of 0.9992 found to closely resemble unity. The values of R<sup>2</sup> and adjusted R<sup>2</sup> depict that there is a very high relationship between the observed and predicted values obtained from the response [23, 25, 23]. **Adequate Precision** measures the signal-to-noise ratio and the present analysis gave adequate precision as 1718.3635 for ash yield which was much higher than the desired value, thereby indicating adequate signals. Thus, values obtained for the models developed can be used to navigate the design space as reported by Agarry and Ogunleye (2012) [26].

The predicted Residual Error Sum of Squares (PRESS) is used in determining the suitability of the model in predicting the responses in new experiments, however, small values are desirable [22]. The PRESS value for ash yield was 5.71 (Table 5) The Coefficient of Variations (CV) obtained for ash yield response of this model is 6.55. CV is the ratio of the standard error of estimate to the mean value of the observed response. It determines the reproducibility of the model this can be estimated when the value is not more than 10 percent [24]. Hence, low values of CV and SD obtained for the ash yield showed the adequacy with which the experiment was conducted.

### **3.5 Diagnostic Case Study for Ash Yield**

The result of diagnostic case studies for the ash yield produced from the combustion of FB, GNS, and kaolin are shown in Table 6, with the actual value representing the yield from the combustion of the biomass from the furnace, while the predicted value present in the standard generated by the software (DOE) used. The closeness of the actual value to the predicted value was indicated by the residual and the straight line in Fig. 2, which shows that R<sup>2</sup> is 1.000. The positive value indicated that the actual value is greater than the predicted value while the negative showed that the predicted value is greater than the actual value. Zero residual values mean that the actual was equivalent to the predicted value on which its comparison was based.

**Table 6. Diagnostic case study for ash yield**

<b>Run Order</b>	<b>Actual Value</b>	<b>Predicted Value</b>	<b>Residual</b>
1	4.90	4.90	0.0001
2	8.15	8.15	-0.0001
3	4.47	4.47	0.0006
4	7.75	7.75	0.0002
5	3.92	3.92	0.0011
6	5.92	5.92	-0.0006
7	5.78	5.78	0.0002
8	7.40	7.40	0.0006
9	2.28	2.28	0.0002
10	7.48	7.48	-0.0012
11	6.10	6.10	0.0006
12	8.35	8.36	-0.0021
13	3.07	3.07	-0.0008
14	3.82	3.82	-0.0011
15	4.24	4.24	-0.0004
16	7.52	7.52	0.0007
17	8.93	8.93	0.0005
19	7.91	7.91	-0.0006
20	7.44	7.44	0.0021

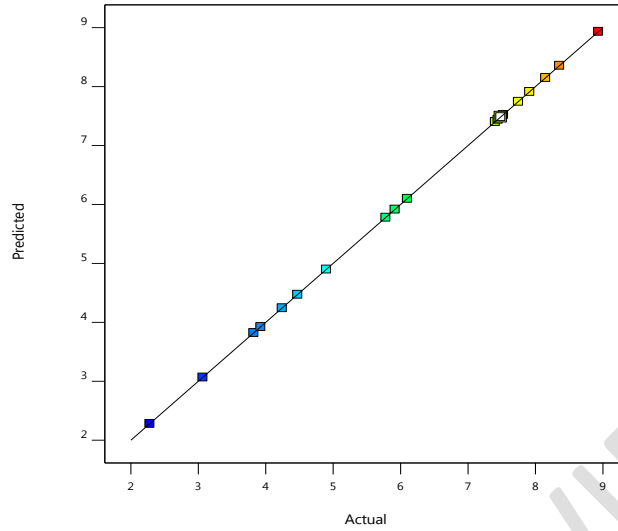


**Fig.2. The plot of predicted vs. actual values for ash yield**

### 3.6 Effects of Interaction of Temperature on Ash Yield

The contour and interaction plots of the factors for the optimization of ash yield are shown in Fig. 3a-b while 3D representations are shown in Fig. 4a-d.

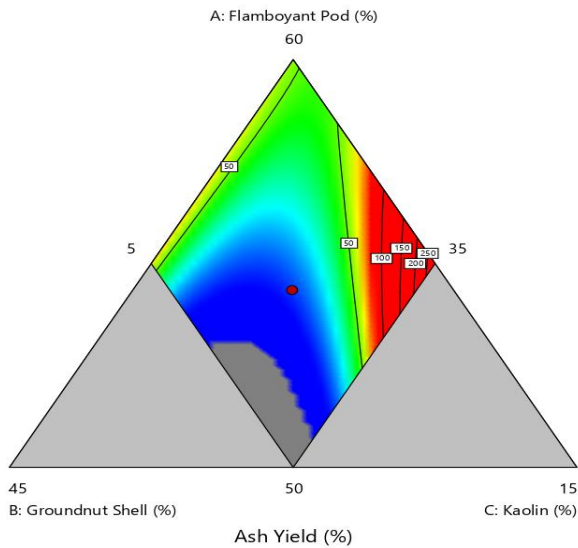


**Fig 3a. Contour plot of ash yield**

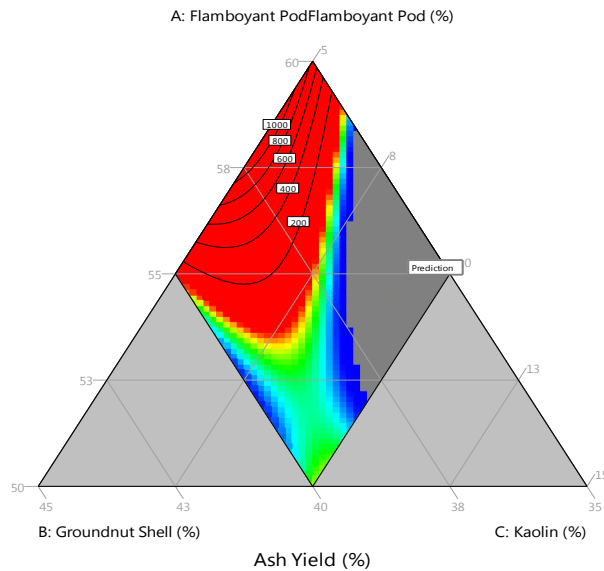
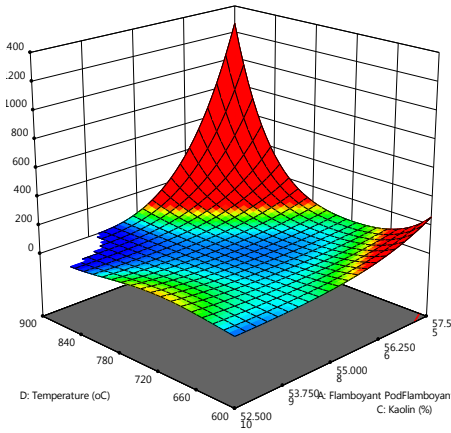
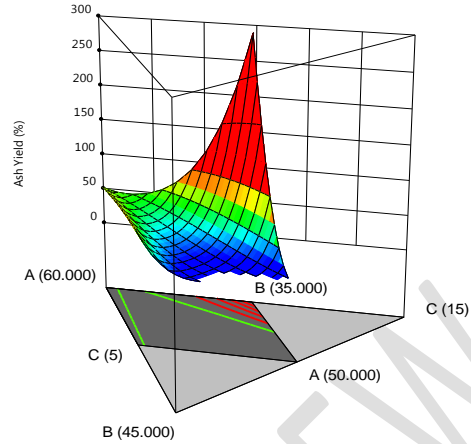


**Fig. 3b. Ternary Contour plot of ash yield**

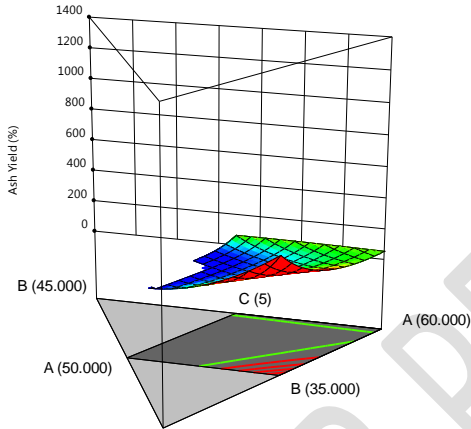
The interaction between temperature and flamboyant pod does not affect the yield (Fig.4a) and a 3D representation of this is shown in Fig. 4d. The interaction of the selected factor (Temperature) on ash yield is shown in Figure 4(a-d) as a contour plot. Contour plots are the graphical representation of the regression equation used to visualize the relationship between the response and experimental levels of each factor. Generally, the contour plots for the three responses indicated that the interaction of temperature affected the ash yield. The corresponding three-dimensional (3D) representations of these trends were illustrated in Figure 3(a-b) for the ash yield. The curves observed in these figures indicated that the model equations were quadratic [23].



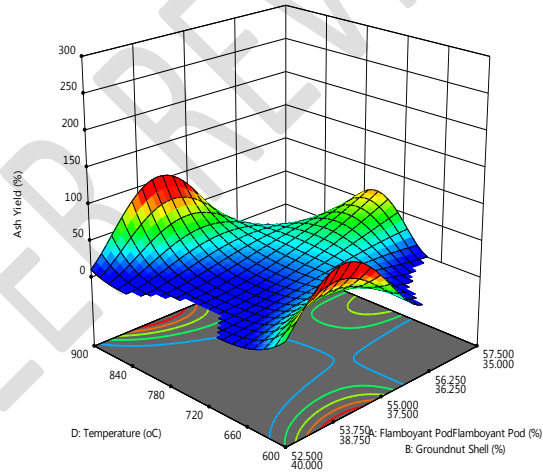
a. 3D plot for Temperature and FB



b. 3D plot for ash yield



c. 3D plot for Temperature and kaolin



d. 3D plot for Temperature and GNS

Fig.4. 3D Representation of interaction of the flamboyant pod, groundnut shell, kaolin and temperature on ash yield

### 3.7 Higher Heating Value

The higher heating values (HHV) (displayed in Table 7) were calculated using Equation (5). From the result, the correlation shows that HHV is higher at low ash yield and lower at higher ash yield which implies that the composition that gives the lowest ash yield will give the higher heating value which makes it best for fuel. This reduction in HHV might be due to the higher inorganic elements in the additives added to the lignocellulosic biomass since these inorganic elements do not contribute to the heating value of the biomass.

Table 7. Proximate analysis and HHV

<b>Samples</b>	<b>Volatile Matter (%)</b>	<b>Fixed Carbon Component (%)</b>	<b>Moisture Content (%)</b>	<b>HHV (MJ/g)</b>
High	4.00	01.84	04.80	12.26
Low	6.00	01.47	03.20	15.14

The experimentation of optimum conditions has led to the realization of the lowest ash yield (5%) and HHV (151.4 kJ/g) (Table 8). In the various models available in the literature to predict HHV from proximate and/or ultimate analyses, one feature that limits their widespread applicability is the range of biomasses used to either determine correlations or train a model. For example, Yin (2011) generated an empirical correlation for the prediction of HHV from both proximate and ultimate analyses of biomass with a mean absolute error of less than 5% [27]. However, their data set comprised biomasses that were predominantly nut/seed shells, fruit stones, straws/grasses, and wood (Table 8).

Zhang et al. (2012) expanded a data set to include a variety of agricultural wastes, food waste, and sludge samples, as done in the present work [28]. Given the greater variety of the biomass represented by Nuchen (2012), it is not surprising that their correlations based on linear relationships between proximate analysis and HHV suffered mean absolute errors of at least 9% and higher and absolute bias errors of up to 4.5% [29]. The study proposed new correlations between FC, VM, and Ash to predict HHV, however, they are linear functions of two and/or three of these biomass descriptors, and as we previously demonstrated in Table 7, the relationships among these variables are not expected to be linear. In the present study, rather than propose and test correlations using such a brute force method, computational modeling was used to train a neural network model to provide a new correlation with improved predictive capabilities over models previously available in the literature which include the correlations from the mixture of two biomass and additive.

**Table 8. Proximate and HHV values compared to literature values for different biomass**

<b>Biomass Materials</b>	<b>Proximate Analysis (%)</b>			<b>Measured HHV (MJ/kg)</b>	<b>References</b>
	FC	VM	ASH		
FB, GNS and Kaolin	01.84	6.00	0.53	12.26	This study
FB, GNS and Kaolin	01.47	4.00	0.56	15.14	This study
Sugarcane Bagasse	13.30	81.50	5.20	17.70	[30]
Corn cob	18.54	80.10	1.36	18.77	[31]
Millet Straw	16.45	78.28	5.27	18.05	[32]
Peanut Shell	13.40	84.90	1.70	18.60	[33]
Wheat Straw	19.80	71.30	8.90	17.51	[28]

### 3.8 The Network Modeling

This study builds upon results presented by Uzoh and Onukwuli (2016) to evaluate its validity as satisfying results of correlation coefficient ( $R^2$ ) [34]. The adequacy of the developed NN model is demonstrated using a scatter plot of the actual and predicted yield shown in Figure 5. The resulting  $R^2$  value of 0.9876 implies a reasonable correlation of all actual experimental data by the proposed model. The plot of ANN predicted and actual ash yield as a result of an error (and the combination of all) (Figure 6). Generally, the ( $R^2$ ) values are used to evaluate the efficiency of the prediction [8].

Figure 5 illustrates Case1 (the most successful testing correlation coefficient with  $R^2 = 0.985$ ) within the ANN model (M 1.1) against the observed data. As shown by the figures, the good predictions of ash characteristics, by using the ANN model (M 1.1), show a good agreement with the observed data. The average correlation coefficient of the ANN model and the observed data is more than 96%. In this way, Case 4 is the best result within this model with 98.7% ( $R^2$ ). Comparing the results of ANN and DOE, the result shows the average prediction of ash yield using the ANN model agrees with the observed data from DOE with an average correlation between the ANN model and the observed data of more than 98%. The  $R^2$  of both is  $>95\%$  which signifies that the model exhibited a successful performance with the correlation coefficient as reported by Khayet and Cojocar, (2012) [35]. The values of training and testing coefficients obtained from the MATLAB toolbox method were 98.57% and 92.94% respectively (Figure 6).

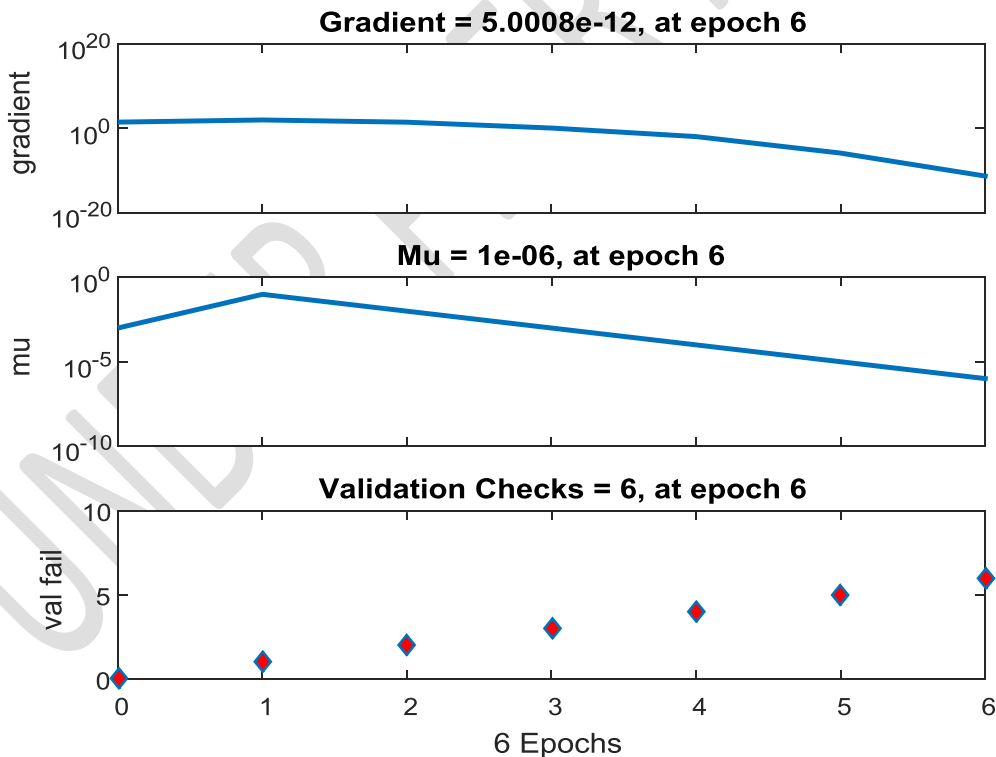


Fig.5. Optimized FFBP-ANN network to predict the ash epoch graph

The ANN was trained through over 1000 epochs with error backpropagation (EBP) training as shown in Fig 6. The correlation between the experimental and ANN predicted ash for training, validation, testing, and overall data sets is shown in Fig. 7. The perfect fit (ANN model prediction equal to experimental data) was shown by the solid line. The proximity of the best linear fit to the perfect fit has been observed, as shown in Fig. 7., which confirms a good correlation between the experimental and the FFBP-ANN [5-6-1] model.

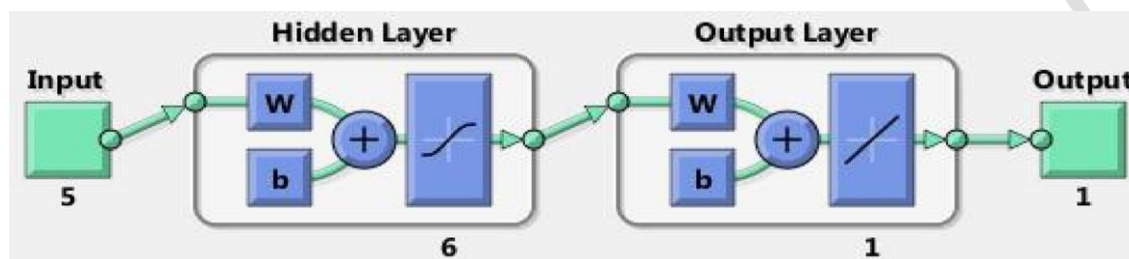


Fig.6. Optimized FFBP-ANN network to predict the ash

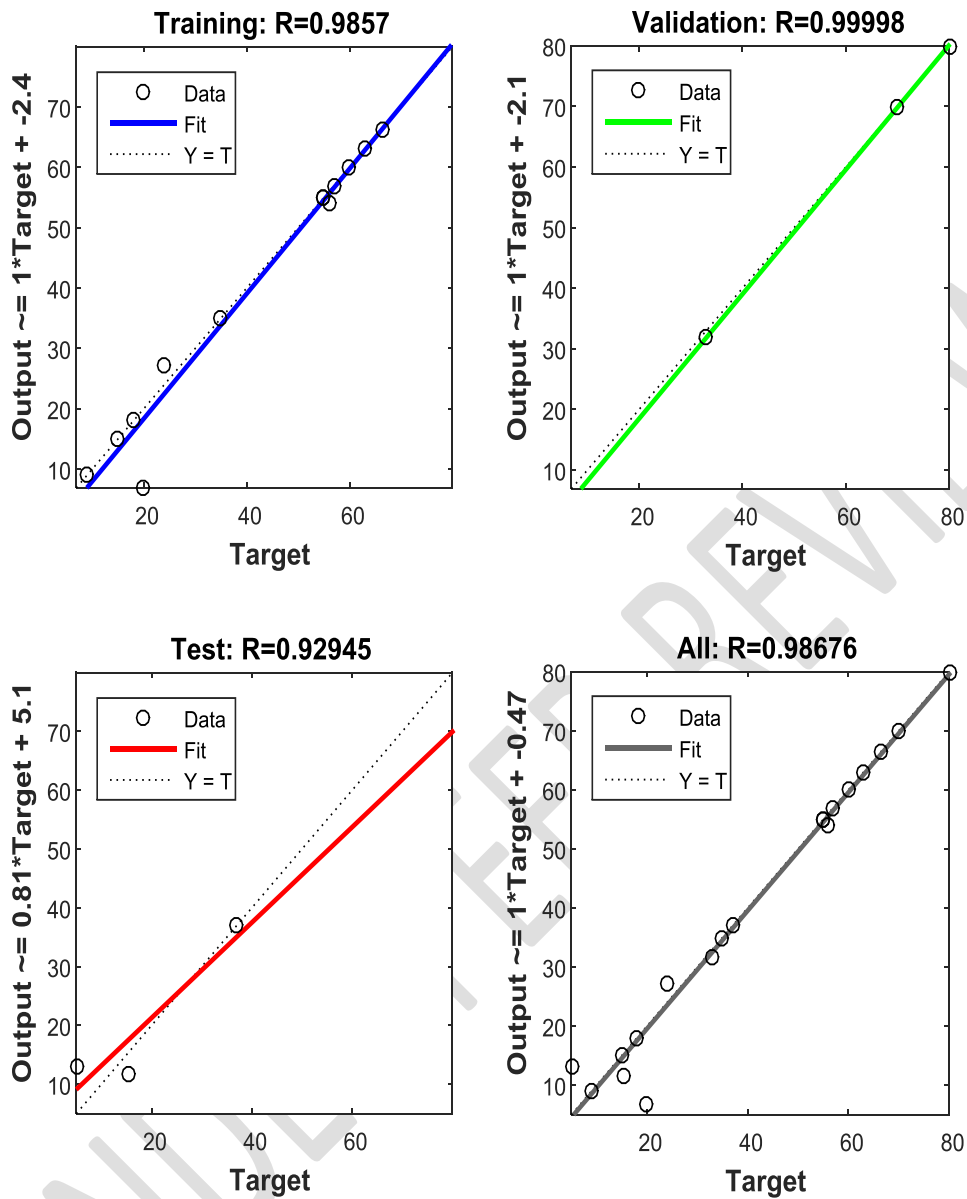


Fig.7.Scatter plots of ANN predicted and actual ash yield

### 3.9 Principal Component Analysis

The result of the principal components analysis shows that of the 20 components, only 5 had extracted eigenvalues over 1 (Table 9). This is based on Chatfield and Collin's assumption which stated that components with an eigenvalue of less than 1 should be eliminated. The extracted 5 components were

subsequently rotated according to varimax rotation to make interpretation easier. The result of rotation revealed further, that the percentages of the total variances of the 5 extracted components when added account for 97.52% (that is their cumulative variance) of the total variance of the observed variables. This indicates that the variance of the observed variables had been accounted for by these 5 extracted components.

**Table 9. Mean square error of the compressed images**

<b>Run</b>	<b>Ash Yield</b>	<b>Eigen Values</b>
1	24	-15.68
2	66	26.72
3	20	-19.68
4	60	20.32
5	15	-24.28
6	35	-4.68
7	33	-6.28
8	55	15.12
9	5	-34.48
10	56	16.32
11	37	-2.48
12	70	30.12
13	9	-30.28
14	15	-25.08
15	18	-21.68
16	57	16.92
17	80	40.12

18	20	-19.68
19	63	22.92
20	55	15.72

### 3.10 Morphology of the Ash Sample

The morphology of the ash as determined by SEM is shown in Fig. 8a-c with 1000x magnification used for all the samples to identify all the morphological properties and larger interactions of the samples in SEM at higher resolution. The samples are discussed in the order of increased dispersion as nondispersive, slightly to moderately dispersive, and dispersive of kaolin in the ash yield, depending on the nature of the morphological features and molecular interactions identified in the SEM images as reported by Larbi and Barati (2011) [36]. It can be seen that the outer surface of the lowest ash yield is smooth (Fig 8a) and its structure is densely covered with orderly bulges which imply that the Sulphur present in kaolin facilitates the sulphonation of alkali chlorides and makes the ashless sticky, as well as increase the melting point of the deposits, thus preventing the slagging/fouling of the heat transfer surface [37]. The massive existence and large size of the materials in the ash, make the pores easy to find by SEM, which is called reticular honeycomb structure [38]. Due to the slight dispersion of kaolin as viewed in Fig 8b, the kaolin was not evenly distributed in the mixture which is the reason why we have higher ash in this mixture compared to the previous run and a similar thing applies to SEM Fig. 8c in which there is no dispersion and this leads to much increase in ash. The temperature has a great impact on the residual carbon content of ash. If the temperature is raised to the decomposition temperature of  $K_2O$ , the unburned carbon surface will get entrapped in the melt. Once carbon is entrapped in the melt, it could be burned completely as it does not have contact with air directly [39].

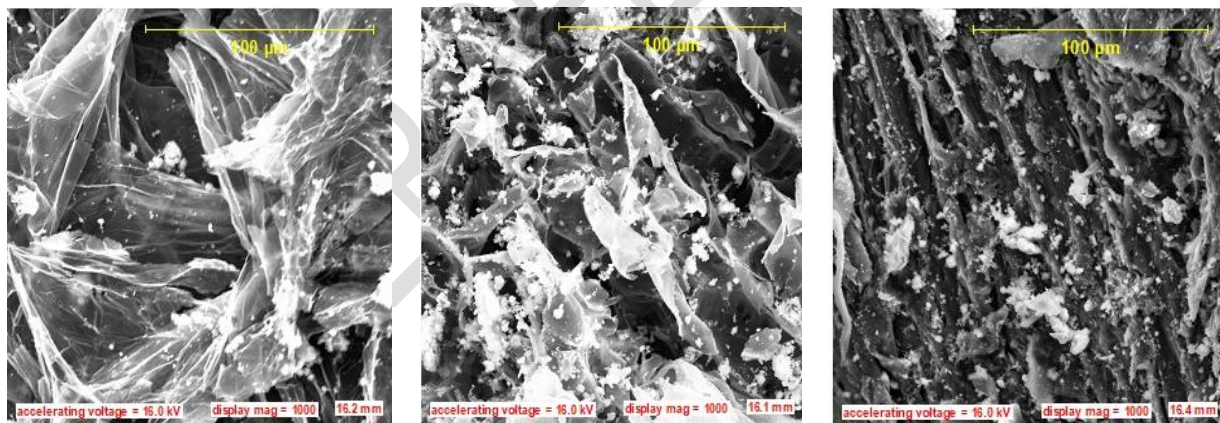


Figure 8. SEM Image of (a) Lowest (b) Medium and (c) Highest Ash yield comparing the dispersability of Kaolin

## 4. CONCLUSIONS

The D-Optimal Design (DOD) was successfully used for the optimization of temperature ( $^{\circ}C$ ) ash yield. This study optimized the combustion characteristics of the mixture of FB, GNS, and Kaolin with respect to ash yield using the DOD of the Design Expert (12.0.1.0) and the laboratory experiment to validate the

process. The result gotten gives the maximum ash yield of 80.8% was obtained from experimental Run 20 (58% FB, 37% GNS, and 5% kaolin at 600 °C), and Run 9 (53% FB, 37% GNS, and 10% kaolin at 825 °C) gives the lowest ash yield. Statistical analysis indicates that the Quadratic model best described the data obtained for three responses ash yield (%). The Error difference obtained between numerical and experimental values was 0.03% for all the selected responses. The experimentation of optimum conditions has led to the realization of the lowest ash yield (5%). Ash yield can be controlled optimally with the use of appropriate additives.

## REFERENCES

1. Dada EO, Alade AO, Adeniji A, Afolabi TJ. Effect of Rice-Bran Pretreatment in Biohydrogen Production Current Journal of Applied Science and Technology. 2021; 40 (16): 12 -19
2. Demirbas A. Combustion characteristics of different Biomass. Progress in Energy and Combustion Science. 2004; 30: 219-230.
3. Goldstein IS. Organic chemicals from biomass. Boca Raton, Florida USA, 1981. <https://doi.org/10.1201/9781351075251>
4. Chin K, Paridah M. Reducing ash-related operation problems of fast-growing timber species and oil palm biomass for combustion applications using leaching techniques. Energy. 2015; 1: 622-630.
5. Dada EO, Awe-Obe UO, Oladosu KO, Alade AO, Afolabi TJ. Optimization of Ash Yield from Bicomposite Biomass (*Terminalia catappa* and *Chrysophyllum albidum*) Seed Barks with Additive upon Combustion. Current Journal of Applied Science and Technology. 2021; 40(22): 26-38. <https://doi.org/10.9734/cjast/2021/v40i2231476>
6. Bernhardt D, Gabauer B. Biogenic residues for the use as wood pellet equivalent fuels. Proceedings of the international conference on thermal treatment Technologies and hazardous waste combustors. 2011; 3: 10-13.
7. Bishnu A, Sanjeev KD, Muhammad Waqas A, Arjun A, Il-Doo K, Dong-Hyun S. Antioxidant activities, polyphenol, flavonoid, and amino acid contents in peanut shell. Journal of the Saudi Society of Agricultural Sciences. 2019; 18(4): 437-442 <https://doi.org/10.1016/j.jssas.2018.02.004>
8. Khan AA, de Jong W, Jansens PJ, Spliethoff H. Biomass combustion in fluidized bed boilers: Potential problems and remedies. Fuel Processing Technology. 2009; 90(1): 21-25. <https://doi.org/10.1016/j.fuproc.2008.07.012>
9. Chin KL, H'ng PS, Maminski M, Go WZ, Lee CL, Raja-Nazrin RA, Khoo PS, Ashikin SN, Halimatun I. Additional additives to reduce ash-related operation problems of solid biofuel from oil palm biomass upon combustion. Industrial Crops and Products. 2018; 123(1): 285-295. <https://doi.org/10.1016/j.indcrop.2018.06.081>
10. Kenechukwu U, Kevin A. Evaluation of Binders in the Production of Briquettes from Empty Fruit Bunches of *Elais guinensis*. International Journal of Sustainable and Green Energy. 2013; 2(4):

176-179.

[https://www.researchgate.net/publication/270706971\\_Evaluation\\_of\\_Binders\\_in\\_the\\_Production\\_of\\_Briquettes\\_from\\_Empty\\_Fruit\\_Bunches\\_of\\_Elais\\_Guinensis](https://www.researchgate.net/publication/270706971_Evaluation_of_Binders_in_the_Production_of_Briquettes_from_Empty_Fruit_Bunches_of_Elais_Guinensis)

11. Adeyanju JA, Ogunlakin GO, Adekunle AA, AlawodeGE, Majekolagbe OS. Optimization of oil extraction from coconut using response surface methodology. *Journal of Chemical and Pharmaceutical Research*. 2016; 8(1):374-381
12. Kareem B, Oladosu KO, Alade AO, Durowoju MO. Optimization of combustion characteristics of palm kernel-based biofuel for grate furnace. *Int J Energy Environ Eng*. 2018; 9:457-472. <https://doi.org/10.1007/s40095-018-0277-5>
13. Bisheswar K, Sucharita S, Gopinath H. *Delonix regia* heterogeneous catalyzed two-step biodiesel production from *Pongamia pinnata* oil using methanol and 2-propanol. *Journal of Cleaner Production* 2020; 255: 120313. <https://doi.org/10.1016/j.jclepro.2020.120313>
14. Pham AD, Dharanipriya P, Bharath KV, Shanmugavadivu M. Groundnut shell -a beneficial bio-waste. *Biocatalysis and Agricultural Biotechnology* 2019; 20: 101206, <https://doi.org/10.1016/j.bcab.2019.101206>
15. ASTM Standard Test Method for Ash in Biomass, ASTM International, West Conshohocken, PA, 2020, [www.astm.org](http://www.astm.org)
16. Tabachnick B, Fidell L. 2013; *Using Multivariate Statistics*. Boston, MA: Pearson Education Inc.
17. Jabeen S, Gao X, Altarawneh M, Hayashi J, Zhang M, Dlugogorski BZ. Analytical Procedure for Proximate Analysis of Algal Biomass: Case Study for *Spirulina platensis* and *Chlorella vulgaris*. *Energy & Fuels*. 2020; 34 (1): 474-482. DOI: 10.1021/acs.energyfuels.9b03156
18. Fakhrur RAA, Suriyati S, Noor-Asma FAS. Estimation of Higher Heating Value of Torrefied Palm Oil Wastes from Proximate Analysis. *Energy Procedia* 2017; 138: 307-312. <https://doi.org/10.1016/j.egypro.2017.10.102>
19. Borrega M, Paarnila S, Greca LG, Jaaskelainen AS, Ohra-aho T, Rojas OJ, Tamminen T. Morphological and wettability properties of thin coating films produced from technical lignins. *Langmuir*. 2020; 36(33): 9675-9684. <https://doi.org/10.1021/acs.langmuir.0c00826>
20. Mohomane SM, Linganiso LZ, Buthelezi T, Motaung TE. Effect of extraction period on properties of sugarcane bagasse and softwood chips cellulose. *Wood Res*. 2017; 62(6): 931-938
21. Katsuya A, Haeyang P, Yasuaki U, Ryo Y. Effect of Mg-based addition to upgraded brown coal on the ash deposition behaviour during combustion. *Fuel*. 2011; 90(11):3230-3236. <http://dx.doi.org/10.1016/j.fuel.2011.06.041>
22. Alade A, Amuda O, Ogunleye O, Okoya A. Evaluation of interaction of carbonization temperatures and concentrations on the adsorption capacities and removal efficiencies of activated carbon using RSM. *Journal of Bioremediation & Biodegradation*. 2012; 3: 1-4.
23. Sumit H, Kumar T, Halder G. Central composite design approach towards optimization of flamboyant pods derived steam activated carbon for its use as heterogeneous catalyst in transesterification of *Hevea brasiliensis* oil. *Energy conversion and management*. 2015; 100: 277-287.

- 24 Montgomery, D. Design and analysis of experiments: Response surface method designs. John Willy and Sons. 2005.101.
- 25 Khani R, Sobhani S, Beyki MB. Highly selective and efficient removal of lead with magnetic nano-adsorbent: Multivariate optimization, isotherm and thermodynamic studies. Journal of colloid and interface science. 2016; 466:198-205. <https://doi.org/10.1016/j.jcis.2015.12.027>
- 26 Agarry SE, Ogunleye OO. Box-Behnken design application to study enhanced bioremediation of soil artificially contaminated with spent engine oil using biostimulation strategy. International journal of energy and environmental engineering. 2012; 3(31), 2012. DOI:10.1186/2251-6832-3-31
- 27 Yin C. Prediction of higher heating values of biomass from proximate and ultimate analysis. fuel. 2011. 90: 1128-1132.
- 28 Zhang Y, Ghaly AE, Li B. Physical Properties of Wheat Straw Varieties Cultivated Under Different Climatic and Soil Conditions in Three Continents. American Journal of Engineering and Applied Sciences. 2012; 5(2): 98-106. <https://doi.org/10.3844/ajeassp.2012.98.106>
- 29 Nhuchhen, D. S. (2012). Estimation of higher heating value of biomass from proximate analysis: a new approach. fuel, 99, 55-63.
- 30 Munir S, Daood S, Nimmo W, Cunliffe A, Gibbs BM. Thermal analysis and devolatilization kinetics of cotton stalk, sugar cane bagasse and shea meal under nitrogen and air atmospheres Bioresource Technology. 2008; 100(3):1413-1418 <https://doi.org/10.1016/j.biortech.2008.07.065>
- 31 Parikh J, Channiwala SA, Ghosal GK. A correlation for calculating HHV from proximate analysis of solid fuels. Fuel. 2005; 84 (5):487-494 <https://doi.org/10.1016/j.fuel.2004.10.010>
- 32 Channiwala SA, Parikh PP. A unified correlation for estimating HHV of solid-liquid and gaseous fuel. Fuel. 2002; 81 (8):1051-1063. [https://doi.org/10.1016/S0016-2361\(01\)00131-4](https://doi.org/10.1016/S0016-2361(01)00131-4)
- 33 Kuprianov VI, Arromdee P. Combustion of peanut and tamarind shells in a conical fluidized-bed combustor: A comparative study. Bioresource Technology. 2013; 140:199-210. <https://doi.org/10.1016/j.biortech.2013.04.086>
- 34 Uzoh FC, Onukwuli DO. Extraction, analysis and desaturation of gmelina seed oil using different soft computing approaches South African Journal of Chemical Engineering, 2016; 22: 6-16. <https://doi.org/10.1016/j.sajce.2016.07.001>
- 35 Khayet M, Cojocaru C. Artificial neural network modeling and optimization of desalination by air gap membrane distillation. Separation and Purification Technology. 2012; 86: 171-182. <https://doi.org/10.1016/j.seppur.2011.11.001>
- 36 Larbi KK, Barati M, Mclean A. Reduction behaviour of rice husk ash for preparation of high-purity silicon. Canadian Metallurgical Quarterly. 2011; 50(4):341-349. <https://doi.org/10.1179/000844311X13117643274677>
- 37 Robinson AL, Junker H, Baxter LL. Pilot-scale investigation of the influence of coal-biomass cofiring on ash deposition. Energy Fuels. 2002; 16(2): 343-355. <https://doi.org/10.1021/ef010128h>
- 38 Bie R, Song X, Liu Q, Ji X, Chen P. Studies on effects of burning conditions and rice husk ash (RHA) blending amount on the mechanical behavior of cement. Cement and Concrete Composites. 2015; 55: 162-168. <https://doi.org/10.1016/j.cemconcomp.2014.09.008>

39 Krishnarao RV, Subrahmanyam J, Kumar TJ. Studies on the formation of black particles in rice husk silica ash. *Journal of European Ceramic society*. 2001; 21(1): 99-104. [https://doi.org/10.1016/S0955-2219\(00\)00170-9](https://doi.org/10.1016/S0955-2219(00)00170-9)

UNDER PEER REVIEW